

## BACKGROUND EVENTS IN MICROCHANNEL PLATES

O.H.W. Siegmund, J. Vallerga, and B. Wargelin  
Space Sciences Laboratory, University of California  
Berkeley, CA 94720

### Abstract

Measurements have been made to assess the characteristics and origins of background events in microchannel plates (MCP's). We have consistently achieved an overall background rate of  $\sim 0.4$  events  $\text{cm}^2 \text{sec}^{-1}$  for MCP's that have been baked and scrubbed. The temperature and gain of the MCP's are found to have no significant effect on the background rate. Detection of 1.46 MeV  $\gamma$  rays from the MCP glass confirms the presence of  $^{40}\text{K}$ , with a concentration of 0.0007% in MCP glass. Furthermore, we show that  $\beta$  decay from  $^{40}\text{K}$  is sufficient to cause the background rate and spectrum observed. Anticoincidence measurements indicate that the background rate caused by cosmic ray interactions is small ( $< 0.016$  events  $\text{cm}^{-2} \text{sec}^{-1}$ ).

### Introduction

There has been considerable speculation<sup>1-5</sup> as to the nature of the intrinsic background in MCP's. Various mechanisms have been suggested as the cause of the intrinsic background including: field emission<sup>3</sup>, cosmic ray interactions<sup>4</sup>, ion feedback, thermionic emission, and radioactivity of the MCP glass<sup>1,2</sup>. Individual background events in MCP's are virtually indistinguishable from events initiated by the interaction of incident radiation with a MCP. Therefore methods such as changing the environmental or operating conditions must be used to investigate the behavior of the intrinsic MCP background. In previous investigations<sup>3,5,6</sup> the results of such tests have often been inconsistent. A recent study<sup>2</sup> has indicated that this may be due to increased background which results from outgassing of MCP's which have not been baked, scrubbed, or kept for a long period under vacuum. Therefore, we have investigated the possible background mechanisms using MCP stacks which have been encapsulated in sealed image tube devices, after undergoing the outgassing processes described. We have assessed the background rate for a wide variation in environmental conditions (temperature, applied field) to ensure that any dependency is clearly visible. The radioactive  $\gamma$  ray decay spectrum from MCP glass has been determined, and we have established quantitative results for the cosmic ray induced background rate.

### General Characteristics of Background Events

The pulse height distribution for background events is markedly different than the amplitude distribution for the detection of photons, or other radiation. Using saturated MCP stacks, in a tandem or Z configuration, it is possible<sup>7</sup> to obtain narrow pulse height distributions for photon initiated events (Figure 1). The photon induced events result in the emission of a photoelectron close to the top of the first MCP in the stack. Thus, the full amplification of the MCP stack is experienced and the saturated pulse height distribution has a gaussian type shape which is well separated from the baseline. We have found that it is possible to obtain narrow distributions as shown in Figure 1 for MCP stacks with total channel length (L) to diameter (D) ratio (L/D) as low as 120:1.

The background event pulse height distribution typically has a negative exponential shape as shown in Figure 2. This is the case even when the MCP's are highly saturated for normal photon counting applications. One simple possible explanation for the shape of the background pulse height distribution is that background events are initiated uniformly throughout the MCP stack. If this is the case background events would be seen at all possible gains. The gain is a rapidly varying function of the depth, from the top surface of the MCP stack, at which the event is generated. We have found that the gain for events initiated at the top of the second MCP in a Z stack is a factor of

10 lower than the full stack amplification. The latter is easily demonstrated by having the photon incident angle parallel to the microchannel pore axis of the first MCP. Assuming a uniform generation of background events along the channels, the rapidly changing gain function will cause the number of background events to increase with decreasing pulse amplitude. Note also in Figure 2 that some background events occur at several times the modal gain amplitude. This indicates that in some cases more than one electron is detected for an individual background event.

Our measurements of the spatial distribution of background events (Figure 3) on quiet MCP stacks show no dependence of the background rate on location. However, some MCP stacks do show enhancement<sup>8</sup> of the background rate at well defined areas. These 'hot spots' are often associated with debris on the MCP surfaces that field emit when charged up. It is frequently possible to determine the loca-

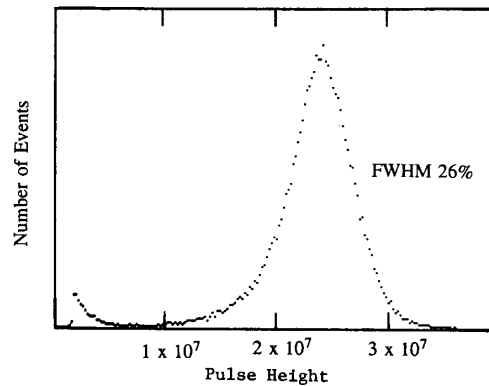


Figure 1. Pulse height distribution for a Z stack of microchannel plates (12.5 $\mu\text{m}$  pores, 240:1 total L/D) irradiated with 2500 $\text{\AA}$  light, modal gain of  $2.4 \times 10^7$ .

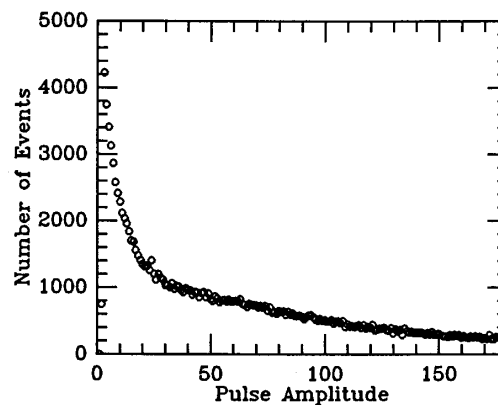


Figure 2. Background event pulse height distribution for a microchannel plate Z stack (12.5 $\mu\text{m}$  pores, 240:1 total L/D, 50mm aperture), gain  $\sim 1.8 \times 10^7$ , 5 hour accumulation. Channel 100 =  $2 \times 10^7 e^-$ .

tion of the debris within the stack from the pulse height distribution of the hot spot events.

The overall background rate<sup>2,7,9</sup> for MCP's which have had extended exposure to atmospheric conditions can be a factor of 10 higher than the best values obtained to date ( $0.4 \text{ events cm}^{-2} \text{ sec}^{-1}$ )<sup>10</sup>. It has been suggested<sup>2</sup> that the outgassing of the channel walls causes the release of ions and neutrals which initiate background events. However, when the MCP's are baked, scrubbed and then kept under vacuum, the background rate decreases and approaches a constant level<sup>1,2,7</sup>. We have also shown<sup>6</sup> that variations in the operating pressure (from  $1.5 \times 10^{-5}$  Torr to  $7 \times 10^{-7}$  Torr) do not affect the background rate. In Figure 4 we present background rate measurements for three MCP Z stacks of the same type of configuration that have undergone preconditioning. The preconditioning consists of baking the MCP's in vacuum to between  $300^\circ\text{C}$  and  $350^\circ\text{C}$  for 8 hours, followed by scrubbing with a high UV flux to extract  $\sim 0.1$  coulombs  $\text{cm}^{-2}$ . Two of the MCP stacks are inside sealed tube devices at  $<10^{-8}$  Torr, while the other is an open face device operated at  $10^{-6}$  Torr. The consistency of the results presented in Figure 4 is significant, considering that the individual MCP stacks possessed different gain and background characteristics when originally delivered. This constant limit to the background event rate in MCP's is the indicator<sup>1</sup> that a fabrication, and time, independent source is responsible for the intrinsic MCP background.

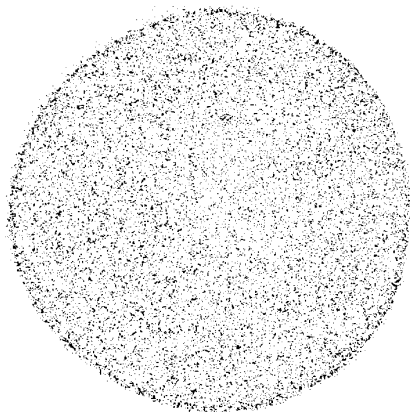


Figure 3. Image of microchannel plate background events for a microchannel plate Z stack ( $12.5\mu\text{m}$  pores, 240:1 total L/D, 50mm aperture), illustrating the overall background uniformity.

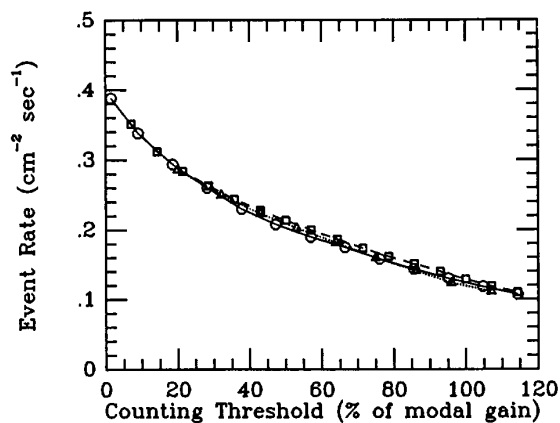


Figure 4. Background event rate as a function of counting threshold for a sample of three preconditioned microchannel plate Z stacks, (all  $12.5\mu\text{m}$  pores, 240:1 total L/D).  
 ○ 25mm sealed tube device, gain  $1.1 \times 10^7$ .  
 □ 40mm sealed tube device, gain  $1 \times 10^7$ .  
 △ 50mm open face detector, gain  $\sim 1.8 \times 10^7$ .

### Thermal Electron Emission

We have previously observed some dependence of the MCP background rate with temperature<sup>5</sup>, although it has also been reported<sup>3</sup> that there is no dependence of the background rate on the temperature. It is important to distinguish the intrinsic background rate of the MCP from effects such as hot spots and outgassing effects. On re-examination of our earlier data<sup>5</sup>, we have found possible hot spot activity in the pulse height distributions for  $50^\circ\text{C}$  and  $22^\circ\text{C}$  that is not present in the  $-10^\circ\text{C}$  data. The MCP stack used was also unbaked and unscrubbed so may have been somewhat gassy.

We have repeated these measurements with a set of MCP's in a sealed tube detector, which have been baked to  $350^\circ\text{C}$ , scrubbed to extract  $0.1$  coul  $\text{cm}^{-2}$ , and are kept at a pressure below  $10^{-8}$  Torr. The detector was operated inside a thermoelectric cooler, and pulse height distributions were accumulated at  $22^\circ\text{C}$ ,  $0^\circ\text{C}$  and  $-15^\circ\text{C}$ . The results (Figure 5) show essentially no difference in the background rate, or spectrum, at these three temperatures.

Metal alloy photocathodes in visible sensitive devices suffer from relatively high background rates due to the thermionic emission of electrons. The emission current density,  $J$ , from a cathode with a thermionic work function,  $\phi$  (eV), is,

$$J = 1.2 \times 10^{-6} T^2 \exp[-\phi/kT] \text{ amps m}^{-2} \quad (1)$$

where  $T$  is the temperature in  $^\circ\text{K}$ , and  $k$  is Boltzmann's constant. In some cases the background event rates exceed  $1000 \text{ cm}^{-2} \text{ sec}^{-1}$  for cathodes with extended red sensitivity (S20). These cathodes have photoelectric work functions, and thermionic work functions, of about  $1.5\text{eV}$  as compared to  $kT = 0.025\text{eV}$  at room temperature. However, blue sensitive photocathodes (bialkali), with work functions of  $\sim 2\text{eV}$ , often have background rates less than  $2 \text{ cm}^{-2} \text{ sec}^{-1}$ . The cooling of cathodes usually results in a drop in the observed background event rate.

If we assume that the MCP glass is an intrinsic semiconductor then  $\phi$  in equation (1) will have a value of  $(E_g + E_a)/2$ , where  $E_g$  is the valence band to conduction band gap energy and  $E_a$  is the electron affinity. The photoelectric work function for MCP glass,  $E_g + E_a$ , may be found from quantum efficiency measurements. From the data of Martin et al<sup>11</sup> we estimate that the photoelectric work function for MCP glass is  $\sim 10\text{eV}$ , thus we expect a thermionic work function of  $\sim 5\text{eV}$ . If this is the case then we expect a negligible background contribution due to thermionic emission in MCP's, from comparisons with bialkali cathodes in Equation (1), which is in accordance with our current observations.

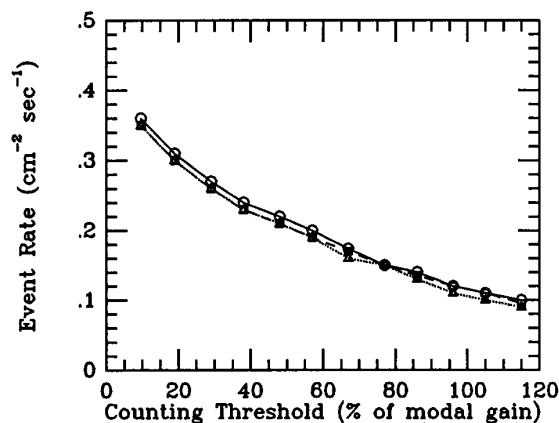


Figure 5. Background event rate as a function of counting threshold for a 25mm sealed tube device with a microchannel plate Z stack at several temperatures (gain  $1.2 \times 10^7$ ,  $12.5\mu\text{m}$  pores, 240:1 total L/D). ○  $-15^\circ\text{C}$ , △  $0^\circ\text{C}$ , □  $22^\circ\text{C}$

### Field Emission

It has been suggested<sup>3</sup> that a significant contribution to the MCP background event rate derives from field emission from structures on the MCP channel walls. If this were the case one might expect to see differences in the background rates of MCP's from different manufacturers or different fabrication batches. However, as we have demonstrated above, the background rates for Mullard MCP's do not seem to vary from batch to batch.

One method of determining the effects of field emission is to vary the voltage applied to MCP's. We typically operate our Z stack MCP's with 1kV to 1.5kV per plate, which is equivalent to an electric field of 1 - 1.5kV mm<sup>-1</sup>. Our earlier results<sup>5</sup> indicated that there was a variation of the background rate as a function of gain, and therefore of applied voltage. We have since remeasured the background event rate as a function of the MCP gain for a sealed tube detector described in the previous section. The results (Figure 6) show a clear change of the MCP background event pulse height spectrum with gain, but do not necessarily infer a different overall background rate. The applied field (gain) ranges from 1406V mm<sup>-1</sup> ( $1.2 \times 10^7$ ), 1281V mm<sup>-1</sup> ( $3.9 \times 10^6$ ), 1200V mm<sup>-1</sup> ( $1.2 \times 10^6$ ), to 1168V mm<sup>-1</sup> ( $3.9 \times 10^5$ ). The overall background event rate for all cases seems to converge to between 0.3 cm<sup>-2</sup> sec<sup>-1</sup> and 0.4 cm<sup>-2</sup> sec<sup>-1</sup> at a low amplitude threshold (~2% of modal gain). However, the background rate at a threshold of 50% modal gain for 1406V mm<sup>-1</sup> is a factor of two higher than the 1168V mm<sup>-1</sup> curve. This behavior suggests that background events are shifted to a higher relative gain as the overall gain is increased, even though the total rate remains constant.

These observations do not agree with the data of Fraser et al<sup>2</sup> which show the opposite dependence of background pulse height spectrum with gain. In the case of our measurements we believe the behavior of the background pulse height distribution to be related to the saturation characteristics of the MCP Z stack. As the applied voltage is increased the MCP stack proceeds into harder saturation, as indicated by the leveling off of the gain-voltage curve<sup>5</sup>. However, the background events are not as highly saturated as the events generated at the front of the first MCP. Thus, they may be considered to lie in the lower gain part of the gain-voltage curve where the slope is greater. If this is so, then any increase in applied voltage will increase the MCP background gain more than the gain increase for events initiated at the MCP input. This would, at least qualitatively, explain the shift of the background pulse height distributions to higher amplitudes relative to the modal gain. Nevertheless, our results do seem to indicate that, over a factor of 30 in MCP gain, there is no significant change in the overall background rate.

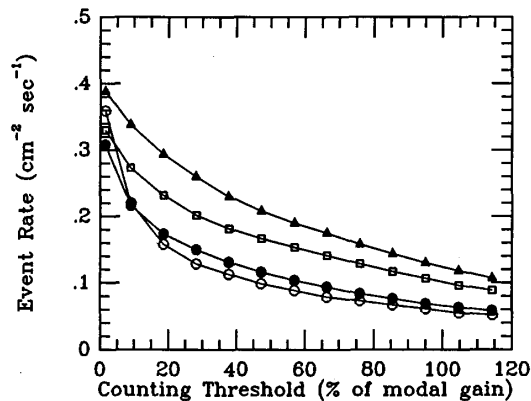


Figure 6. Background event rate as a function of counting threshold for a 25mm sealed tube device with a microchannel plate Z stack, (12.5 $\mu$ m pores, 240:1 total L/D), at various gains.  $\blacktriangle$  gain  $1.2 \times 10^7$ ,  $\square$  gain  $3.9 \times 10^6$ ,  $\bullet$  gain  $1.2 \times 10^6$ ,  $\circ$  gain  $3.9 \times 10^5$ .

### Cosmic Ray Induced Events

The passage of cosmic rays through a channel plate is likely to result in an ionization track, from which some electrons may be detected. However, the flux of cosmic rays at the Earth's surface is not high enough to produce the background rate observed for MCP's. The total cosmic ray flux crossing unit horizontal area is approximately 0.024 events cm<sup>-2</sup> sec<sup>-1</sup><sup>12</sup>, of which ~75% are muons. This rate is at least a factor of 20 lower than the observed MCP background rate even if we assume 100% detection efficiency for the cosmic rays. Also, Fraser et al<sup>2</sup> have estimated that the cosmic ray flux is ~0.0178 events cm<sup>-2</sup> sec<sup>-1</sup> for a horizontal surface, and ~0.014 events cm<sup>-2</sup> sec<sup>-1</sup> for a vertical surface. A previous experiment<sup>3</sup> used a plastic scintillator to determine the number of MCP background events that were coincident with cosmic ray events. The conclusion was that less than 5% of the MCP background events were attributable to cosmic rays.

We have used a plastic scintillator well (18cm x 18cm cylinder, with a 10cm x 10cm well) to determine the coincidence rate and the MCP pulse height spectrum for cosmic ray events. The scintillator well was painted with a reflective MgO layer, and was viewed with an 18cm photomultiplier tube (EMI9623B). A sealed tube MCP detector<sup>13</sup> (25mm aperture, MCP Z stack with 12.5 $\mu$ m channels and 240:1 L/D) was placed into the scintillator well. Signals from the MCP detector and the photomultiplier were amplified (Canberra 2004 + 2022) and passed through single channel analysers (Ortec 551) with the subsequent signals being sampled by a universal coincidence unit (Ortec 418A). Any output pulse from the coincidence unit implies that events occurred simultaneously in the MCP and scintillator. This coincidence signal was used to gate an Ortec-Norland 5510 multichannel analyser, which was configured to accumulate a pulse amplitude distribution of the amplified MCP detector signals. Discrimination levels were set at low amplitudes (~50mV) but well above the noise levels, and the pulse synchronization was carefully adjusted to provide the correct gate delay time.

Figure 7 shows the MCP detector pulse height distribution for events that are coincident with cosmic ray event detections in the plastic scintillator. This may be compared with the total background event pulse height distribution (Figure 8) and the single photoelectron pulse height distribution (Figure 9) of the detector. The overall rate for the cosmic ray event component of the MCP background is found to be 0.0157 events cm<sup>-2</sup> sec<sup>-1</sup>. In this case the MCP detector was placed in a horizontal orientation (the normal to the MCP is vertical). The pulse height distribution for the events that are coincident with cosmic rays when the MCP detector was placed vertically is shown in Figure 10. The total coincident background event rate in the latter case is 0.00848 events cm<sup>-2</sup> sec<sup>-1</sup>. These results indicate that only 4% of MCP background events are caused by cosmic rays for a horizontal MCP orientation, and ~2.2% for a vertical MCP orientation.

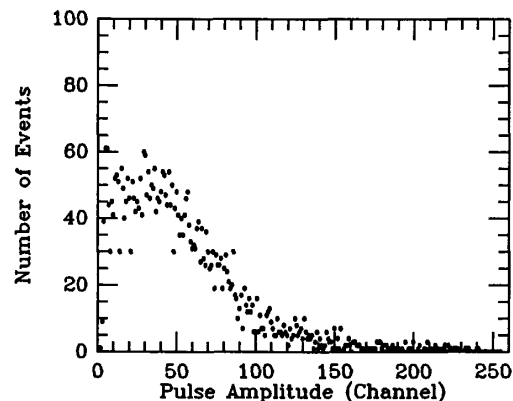


Figure 7. Background pulse height distribution, of events coincident with cosmic ray induced signals in a plastic scintillator shield, for a horizontal microchannel plate Z stack (12.5 $\mu$ m pores, 240:1 total L/D, 25mm aperture), gain  $\sim 1 \times 10^7$ , 14 hour accumulation. Channel 100 =  $2 \times 10^7$  e<sup>-</sup>.

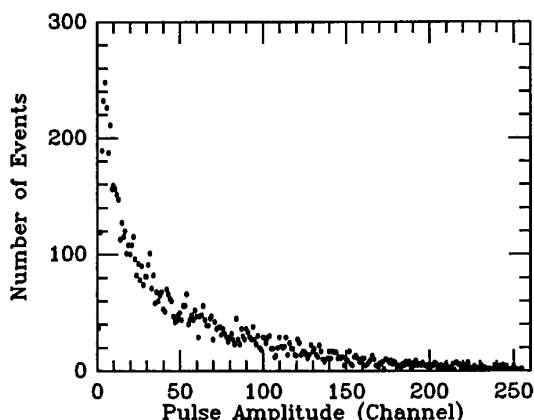


Figure 8. Background event pulse height distribution for a microchannel plate Z stack (12.5 $\mu$ m pores, 240:1 total L/D, 25mm aperture), gain  $\sim 1 \times 10^7$ , 1.1 hour accumulation. Channel 100 =  $2 \times 10^7 e^-$ .

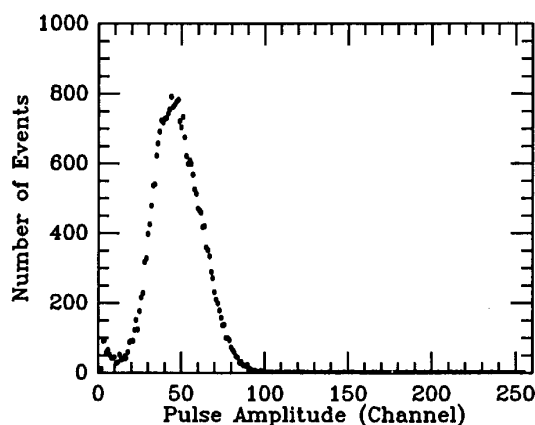


Figure 9. Single photoelectron pulse height distribution for a microchannel plate Z stack (12.5 $\mu$ m pores, 240:1 total L/D, 25mm aperture), gain  $\sim 1 \times 10^7$ . Channel 100 =  $2 \times 10^7 e^-$ .

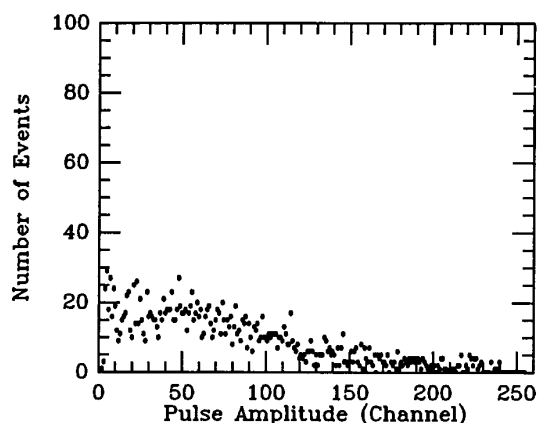


Figure 10. Background pulse height distribution, of events coincident with cosmic ray induced signals in a plastic scintillator shield, for a vertical microchannel plate Z stack (12.5 $\mu$ m pores, 240:1 total L/D, 25mm aperture), gain  $\sim 1 \times 10^7$ , 14 hour accumulation. Channel 100 =  $2 \times 10^7 e^-$ .

We have estimated the total incident flux in the laboratory from the event rate seen in the plastic scintillator. With the scintillator in a horizontal position (effective area 248 cm<sup>2</sup>) we obtain a rate of 5.8 events sec<sup>-1</sup> and with the scintillator placed vertically (effective area 316 cm<sup>2</sup>) we get a rate of 7.5 events sec<sup>-1</sup>. Both these values imply a total flux of  $\sim 0.0235$  events cm<sup>-2</sup> sec<sup>-1</sup>, assuming 100% scintillator detection efficiency, which is very close to the cosmic ray flux expected at sea level. Note that these measurements were made on the second floor of a three story building at an altitude of about 300m. We also deduce that the MCP (3mm deep stack) detection efficiency for cosmic rays is of the order 65% from the above measurements, which is comparable with the efficiency measured for other relativistic charged particles<sup>14</sup>.

The pulse height distributions for cosmic ray induced events in the MCP stack are quite different from the bulk of background events. Also the distributions for the two MCP orientations are different. When the MCP stack is placed vertically there are more cosmic ray tracks parallel to the MCP surface. The cosmic ray flux maximizes at the zenith, and has a  $\cos^2\theta$  dependence. Thus when the MCP is placed vertically the rate will be lower, but will also extend to a greater pulse amplitude. The mean cosmic ray muon energy is  $\sim 2$  GeV, giving an energy loss (dE/dx) of  $\sim 5$  MeV/cm in MCP glass. We estimate that between 3 and 12 electrons are detected over the depth of the MCP stack for a typical cosmic ray muon event entering the stack between the normal and 45° to the normal. This assumes values of 10eV for the MCP work function, 33Å for the secondary electron diffusion length, and 0.15 for the electron escape probability at the channel wall surface<sup>2</sup>. The number of electrons detected roughly correlates with the pulse height spectrum of cosmic ray induced background events in MCP (Figure 9), which extends to  $\sim 5x$  the modal gain although most events occur below 2x the modal gain. However, a detailed model is required to predict the effect of the position (and therefore gain) and number of electrons detected on the pulse height distribution.

#### Radioactive Decay Events

The inclusion of potassium in MCP glass suggests that some MCP background events may originate from the radioactive decay of <sup>40</sup>K. <sup>40</sup>K exists in potassium at a level of 0.0118%, and emits  $\beta$  and  $\gamma$  radiation. The  $\beta$  (1.32 MeV) decay has a half life of  $1.43 \times 10^9$  years, and the  $\gamma$  decay (1.46 MeV) has a half life of  $1.2 \times 10^{10}$  years<sup>15</sup>. Approximately 89.3% of the decays are by  $\beta$  emission. To determine the decay rate for a typical MCP we must determine the potassium content.

We have measured the radioactive decay rate of a microchannel plate by placing it in a germanium well counter. The  $\gamma$  ray energy spectrum obtained was integrated for 100 hours, and an empty well background was subtracted from this data. The resulting spectrum shows that the major decay components are 1.46 MeV  $\gamma$  rays from <sup>40</sup>K and 352 KeV  $\gamma$  rays from <sup>226</sup>Ra. The flux of the latter is a factor of 17 lower than the <sup>40</sup>K  $\gamma$  flux. This predicts that uranium exists in the MCP glass at a level of  $\sim 0.9$  ppm. Comparing the 1.46 MeV  $\gamma$  decay rate with that of a control sample of KCl we estimate that MCP glass contains 6.07% by weight of potassium.

The total <sup>40</sup>K content of the MCP used (60mm diameter, 1mm thick, weight 2.97gm) is 21.2 $\mu$ gm, which has a specific activity of 0.23 disintegrations sec<sup>-1</sup>  $\mu$ gm<sup>-1</sup> for  $\beta$  decay<sup>15</sup>. This infers a total rate of 4.88  $\beta$  decays sec<sup>-1</sup> for the entire plate, or 0.17 decays cm<sup>-2</sup> sec<sup>-1</sup>, which is comparable with the value calculated by Fraser et al<sup>2</sup>. For a three MCP stack this would result in 0.52 decays cm<sup>-2</sup> sec<sup>-1</sup>, which is close to the observed MCP background rate. We must, however, determine the detection efficiency for the radioactive decay components to obtain an event rate for the decay induced background.

The absorption coefficient of materials at 1.46 MeV is almost independent<sup>16</sup> of the material, and has a value of  $\sim 0.06$  cm<sup>2</sup> gm<sup>-1</sup>. We estimate that the  $\gamma$  rays have a 1/e attenuation length of about 5cm in solid MCP lead glass, so less than 2% of the  $\gamma$  rays would be stopped by passing through the entire MCP stack 3mm thick. Assuming the detection efficiency for  $\gamma$  rays is less than 2%, the 1.46 MeV  $\gamma$

ray induced background is negligible compared to the  $\beta$  decay rate. For the uranium in the MCP the total specific activity is  $0.01 \text{ decays } \mu\text{gm}^{-1} \text{ sec}^{-1}$ , which corresponds to  $\sim 0.027 \text{ decays sec}^{-1}$ , and is therefore two orders of magnitude lower than the expected  $^{40}\text{K}$   $\beta$  rate.

The practical range of the 1.32 MeV  $\beta$ 's is approximately  $581 \text{ mg cm}^{-2}$ , which corresponds to a range of 2.2mm in MCP glass (density  $2.6 \text{ gm cm}^{-3}$ ). The  $\beta$  range in an MCP with a channel area of 60% is then  $\sim 5.5\text{mm}$ . The  $dE/dx$  value for the 1.46 MeV  $\beta$ 's can be shown to be  $\sim 4 \text{ MeV cm}^{-1}$  for MCP glass. Performing a similar calculation to that done for cosmic ray events we conclude that a  $\beta$  decay track through the MCP stack would produce between 2 and 10 detected electrons (for angles from normal to  $45^\circ$  to the normal). Events produced in the bottom MCP will not have sufficient amplitude to be detected in the pulse height distribution. However, assuming that the  $\beta$  detections in the bottom plate are less than half the single MCP decay rate, and a similar amount for other geometrical losses, we estimate a total  $\beta$  induced background rate of between 0.52 and  $0.34 \text{ events cm}^{-2} \text{ sec}^{-1}$ . These events would mainly look like single electron detections throughout the MCP stack, but a few would give larger events up to  $\sim 10\times$  the modal gain. This seems to correlate quite well with the observations described above.

#### Discussion

From the data presented above, and the conclusions of Fraser et al.<sup>2</sup>, it is clear that the main source of background events in preconditioned MCP's is the  $\beta$  decay of  $^{40}\text{K}$  in the MCP glass. Since these background events normally release only a few electrons into the MCP channels it is unlikely that many can be rejected on the basis of extended event track length. The most effective way to reduce the MCP background would be to remove the  $^{40}\text{K}$ , or remove all the potassium from the MCP glass.<sup>2</sup> The dominant background component would then be the cosmic ray induced events, with rates of  $< 0.016 \text{ events cm}^{-2} \text{ sec}^{-1}$  at sea level. Experience with MCP's in satellite instruments indicates that the overall background event rate increases in orbit. In the case of ECOM-721 the rate increased from  $\sim 0.55 \text{ events cm}^{-2} \text{ sec}^{-1}$  in the laboratory to  $\sim 0.7 \text{ events cm}^{-2} \text{ sec}^{-1}$  in a 600 km polar orbit. For the EXOSAT CMA<sup>17</sup> and HEAO-B HRI<sup>3</sup> the background rates increased by a factor of  $\sim 2$ . These increases may not be completely due to the increase in cosmic ray flux, but they do indicate that there is profit in removing the  $^{40}\text{K}$  background component. If this is complemented by the use of anticoincidence techniques, as employed in these studies, a significant decrease in the in orbit MCP background rate may be achievable.

#### Acknowledgements

We would like to thank Professor S. Bowyer and Dr. M. Lampton for stimulating discussions on this work, D. Liedahl, J. Sokolowski and T. Stevens for their participation in setting up the experiments, Dr. S. Chakrabarti and Dr. C. Hailey for the use of the sealed tube MCP devices, and A. Smith for making the radioactive analysis of MCP glass. This work was supported by grant# NGL05-003-497.

#### References

- 1) G.W. Fraser, M.J. Whiteley and J.F. Pearson, "Developments in microchannel plate detectors for imaging X-ray astronomy," SPIE Vol. 597, 343-351, 1985.
- 2) G.W. Fraser, J.F. Pearson, and J.E. Lees, "Dark noise in microchannel plate X-ray detectors," Nucl. Instrum. Meth. Vol. A254, 447-462, 1987.
- 3) J.P. Henry, E.M. Kellogg, U.G. Briel, S.S. Murphy, L.P. Van Speybroeck and P. Bjorkholm, "High resolution imaging X-ray detector for astronomical measurements," SPIE, Vol. 106, 163, 1977.
- 4) J.G. Timothy, "Curved channel microchannel array plates," Rev. Sci. Instrum. Vol. 52, 1131-1142, 1981.
- 5) O.H.W. Siegmund, K. Coburn and R.F. Malina, "Investigation of large format microchannel plate Z configurations," IEEE, Trans. Nucl. Sci. NS-32, 443-447, 1985.
- 6) O.H.W. Siegmund, R.F. Malina, K. Coburn and D. Werthiemer, "Microchannel plate EUV detectors for the extreme ultraviolet explorer," IEEE, Trans. Nucl. Sci. NS-31, 776-779, 1984.
- 7) O.H.W. Siegmund, M. Lampton, S. Chakrabarti, J. Vallerger, S. Bowyer, and R.F. Malina, "Application of Wedge and Strip image Readout Systems to Detectors for Astronomy," SPIE, Vol. 627, 660-665, 1986.
- 8) O.H.W. Siegmund, M. Lampton, J. Bixler, J. Vallerger and S. Bowyer, "High efficiency photon counting detectors for the FAUST spacelab far ultraviolet astronomy payload," IEEE Trans. Nucl. Sci. NS-34, 41-45, 1987.
- 9) M.J. Whiteley, J.F. Pearson, G.W. Fraser and M.A. Barstow, "The stability of CsI coated microchannel plate array x-ray detectors," Nucl. Instrum. Meth. Vol. 224, 287, 1984.
- 10) O.H.W. Siegmund, M. Lampton, J. Bixler, S. Chakrabarti, J. Vallerger, S. Bowyer and R.F. Malina, "Wedge and strip image readout systems for photon counting detectors in space astronomy," Journal of the Optical Society of America - A, Vol. 3, 2139-2145, 1986.
- 11) C. Martin, S. Bowyer, "Quantum efficiency of opaque CsI photocathodes with channel electron multiplier arrays in the extreme and far ultraviolet," Appl. Opt. Vol. 21, 4206, 1982.
- 12) Review of Particle Properties, Rev. Mod. Phys. Vol. 56(2), S49-S54, 1984.
- 13) S. Chakrabarti, O.H.W. Siegmund, and J. Hecht, "Continuous readout photon counting imaging detector," Accepted for publication in SPIE, Vol. 834, 1987.
- 14) K. Oba, P. Rehak, and S.D. Smith, "High gain microchannel plate multipliers for particle tracking or single photoelectron counting," IEEE Trans. Nucl. Sci. NS-28, 705-711, 1981.
- 15) E. Browne, J.M. Dairiki, and R.E. Doebler, Table of Isotopes, New York, Wiley Interscience, 1978.
- 16) M.V. Zombeck, Handbook of Space Astronomy and Astrophysics, Cambridge, Cambridge University Press, 1982.
- 17) I.M. Mason, G. Branduardi-Raymont, J.L. Culhane, R.D.H. Corbet, J.C. Ives, and P.W. Sanford, "The EXOSAT imaging X-ray detectors," IEEE Trans. Nucl. Sci. NS-31, 795-800, 1984.